Electronic Supplementary Material (ESI) for Physical Chemistry Chemical Physics.
This journal is © the Owner Societies 2019

Electronic Supplementary Information (ESI)

Activation of CO_2 at the electrode-electrolyte interface by a co-adsorbed cation and an electric field

Irina V. Chernyshova,[a,b] *and Sathish Ponnurangam*[c]

[a] Department of Earth and Environmental Engineering, Columbia University, New York, NY, United States
[b] Department of Geoscience and Petroleum, Norwegian University of Science and Technology, Trondheim, Norway
[c] Department of Chemical and Petroleum Engineering, University of Calgary, Calgary, Alberta, Canada

Table S1. Effect of relaxation of the topmost Cu(111) surface layer on the geometry and binding energy of $*CO_2^-$ in (CO_2-$Na_{on\ top}$)

	Frozen	Relaxed 1st Cu(111) layer
Bond length, Å		
C–O_1	1.25	1.26
C–O_2	1.35	1.33
C–Cu	1.97	1.97
O_2–Cu	2.06	2.06
Cu_C…Na	4.50	4.49
C…Na	2.55	2.53
O_1…Na	2.23	2.22
O-C-O angle (°)	119.5	120.4
Binding Energy, eV, eqn (4)	–1.51	–1.57

S1. Additional DFT data

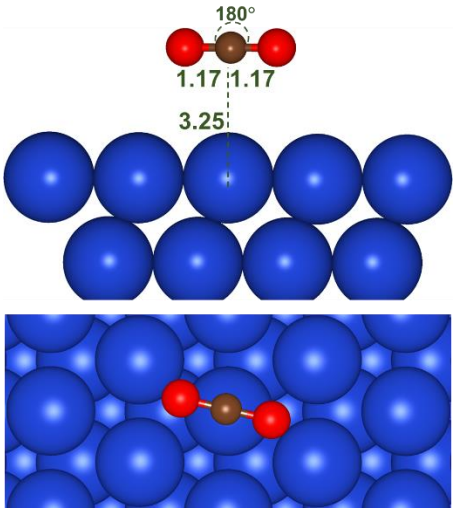

Figure S1. The relaxed structure of CO_2 interacting with clean Cu(111). Top panel=side view. Bottom panel=top view. Atom colors: dark blue – Cu, red – oxygen, brown – carbon.

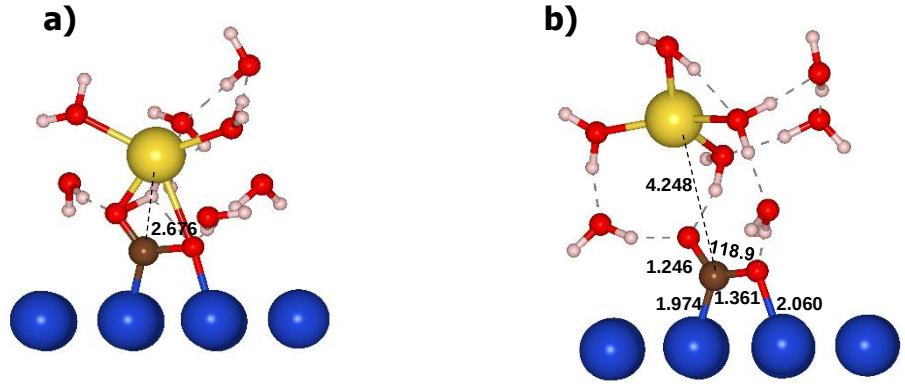

Figure S2. (**a**) The initial structure of the hydrated $*CO_2^-$…Na^+ *contact ion pair* which was constructed by flipping the hydrated Na^+ cation in the relaxed (CO_2-$Na_{on\text{-}top}$+8H_2O) (**Figure 1d**). (**b**) A *hydration-shared ion pair* resulted from relaxation of structure (a). Atom colors: dark blue – Cu, red – oxygen, brown – carbon, yellow – sodium.

S2. Electronic properties of physisorbed CO_2 and free $CO_2^{\bullet-}$ anion radical

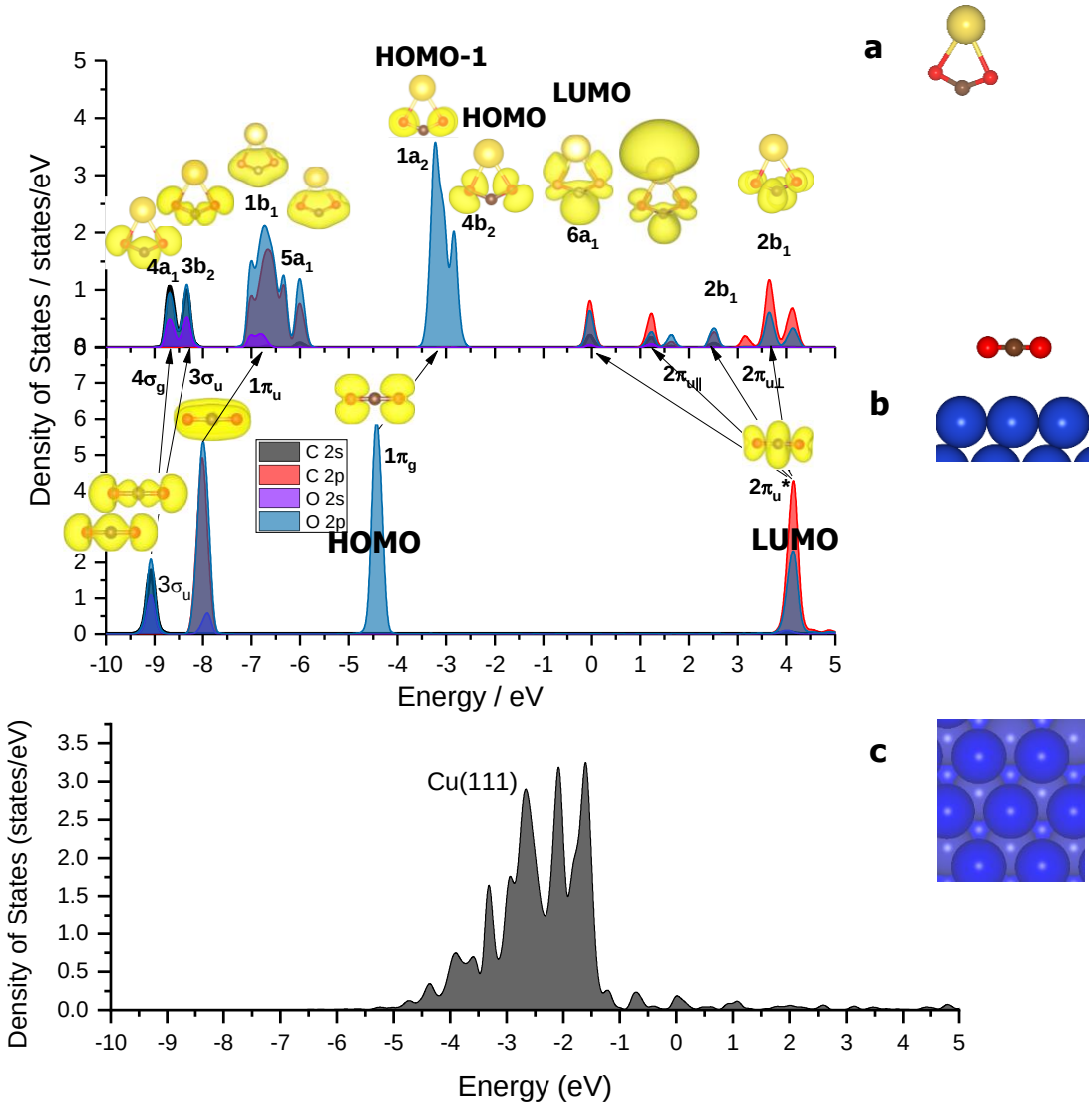

Figure S3. Projected density of states (pDOS): (**a**) on the C and O valence atomic orbitals of a free anion radical modelled as a CO_2-Na ionic pair. (**b**) on the C and O valence atomic orbitals of CO_2 physisorbed on Cu(111), and (**c**) Cu d states of Cu(111) surface. Panels **a** and **b** also show the electronic density isosurfaces of the molecular orbitals. Zero energy position represents the Fermi level. Color code: red=oxygen, brown=carbon, green=sodium.

Below we briefly survey the geometric and electronic properties of two reference states—linear ($D_{\infty h}$) CO_2 molecule physisorbed on Cu(111) and free $CO_2^{\bullet-}$ anion radical (C_{2v}). Physisorbed

CO_2 was simulated by placing a linear CO_2 molecule over the Cu(111) surface. Its geometry is negligibly perturbed as compared to free CO_2 in vacuum, in agreement with the prior results.[1-2] Free $CO_2^{\bullet-}$ radical was modelled by relaxing a CO_2 molecule activated by Na in vacuum. In the radical, CO_2 accepts $-0.9|e|$ acquiring a bent geometry with the O-C-O angle of 134°, while the length of its C-O bonds increases from 1.17 Å to 1.25 Å. These geometric characteristics are close to the corresponding experimental and theoretical values reported for free $CO_2^{\bullet-}$.[3-4] The geometries and Bader charges of these two reference systems are summarized in **Table 1**.

Below we analyze the density of states projected on the atomic orbitals (pDOS) of CO_2 and $CO_2^{\bullet-}$. To visualize the molecular orbitals that predominantly contribute to the pDOS peaks, we calculated the 3D electron density plots for each peak and added these plots to the pDOS graph (**Figure S3**). The frontier molecular orbitals (closest to the Fermi level) of the physisorbed CO_2 molecule present two sets of π orbitals. The HOMO is the degenerate lone pair ($n\pi$) centered on the O atoms, $1\pi_g$, while the LUMO is the doubly degenerate C-O antibonding $2\pi_u^*$ orbital. These frontier orbitals are most important for the CO_2 coordination to metal atoms in molecular complexes.[5-7] This electronic structure allows CO_2 to act *simultaneously* as electron acceptor on $2\pi_u^*$ and donor from $1\pi_g$, which can be behind the versatility of adsorbed CO_2 as the reaction intermediate.

The degeneracy of the π orbitals of CO_2 is lifted in $CO_2^{\bullet-}$ radical (**Figure S3**). These orbitals are split into two components—perpendicular and parallel to the $CO_2^{\bullet-}$ plane. In particular, the $1\pi_g$ orbital (HOMO) is split into the $1a_2$ (perpendicular) and $4b_2$ (parallel) components, while $2\pi_u^*$ (LUMO) splits into $2b_1$ (perpendicular) and $6a_1$ (parallel). Importantly, all the CO_2 orbitals are destabilized except for LUMO which is stabilized. The $2b_1$ component of LUMO is stabilized only by 1.5 eV and remains unoccupied (above the Fermi level). The stabilization is more pronounced for the $6a_1$ component. This orbital downshifts by ca. 4 eV to the Fermi level, which corresponds to its occupation in the radical by almost one electron. The electron transfer to the $6a_1$ orbital drives bending of the linear CO_2 molecule and elongates (activates) its bonds, which minimizes the electron repulsion within the $6a_1$ orbital, as well as molecular energy.

S3. Additional pDOS data

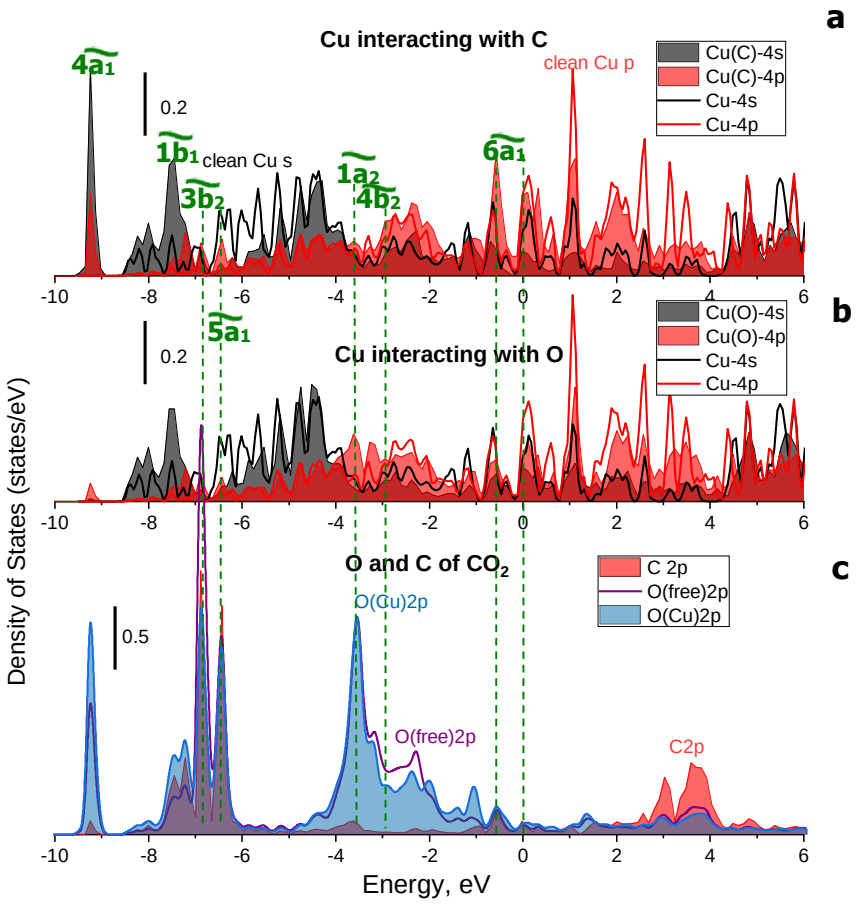

Figure S4. pDOS of (CO_2-$Na_{on\ top}$)/Cu(111): (**a,b**) projected on the Cu 4s and Cu 4p states of the *CO_2^-coordinating Cu atoms of Cu(111) as compared to clean Cu(111) and (**c**) C 2p and O 2p states of *CO_2^-. The common states are shown by vertical dashed lines.

Figure S4 shows that Cu sp electrons are mixed with C 2p and O 2p electrons of *CO_2^- (these pDOS have common resonances).

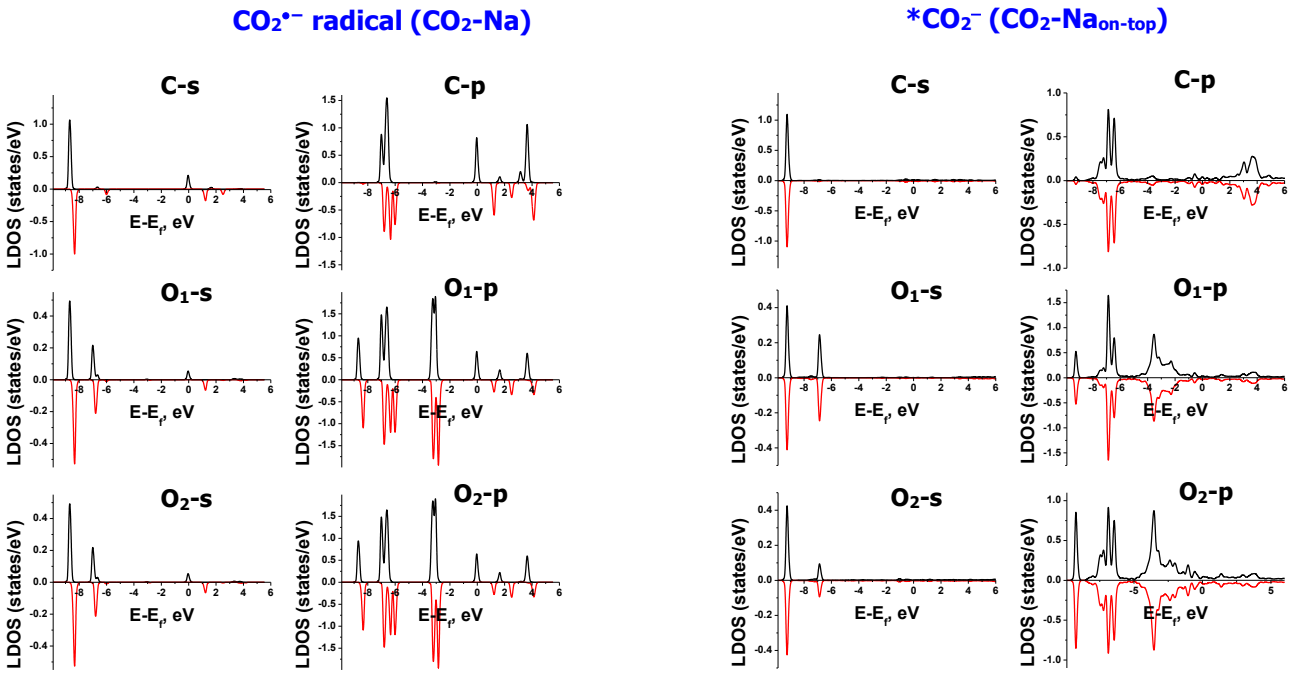

Figure S5. Local density of (black) spin-up and (red) spin-down states projected on O 2s, O 2p, C 2s, and C 2p of (*left panel*) free $CO_2^{\bullet-}$ anion radical modelled as CO_2-Na ionic pair and (*right panel*) adsorbed CO_2 modelled as (CO_2-$Na_{on\text{-}top}$).

The left panel of **Figure S5** shows that the spin-up and spin-down states of $CO_2^{\bullet-}$ have different energy, which results from their different polarization due to the presence of an unpaired electron density. In contrast, the states of adsorbed carboxylate (right panel) are fully symmetrical with respect to the x axis, which indicates that its electrons are paired (the shell is closed). Hence, this species is not a radical.

Figure S6 compares Cu d pDOS of the Cu atoms coordinating $*CO_2^-$ with those of the clean Cu(111) surface. In agreement with the charge redistribution plots (**Figure 3**), it shows that most strongly interacting with CO_2 are the d_{z2} states of the Cu atom coordinating the C atom interact. This conclusion follows from the largest downshift of the corresponding d_{z2} states (due to their interaction with the O lone-pair electrons) and the most pronounced spreading of these

states across the Fermi level. Both the stabilization and the presence at the Fermi level are weaker for the d_{z2} states of the Cu atom coordinating the O atom of $*CO_2^-$ (**Figure S6c**). In addition, these d_{z2} states of the Cu atom coordinating the O atom display pronounced resonances at −1.4 and −1.1 eV assigned to the $4\widetilde{b_2}^*$ antibonding states (hybridization of the d_{z2} states with the in-plane O lone pair ($4b_2$) of $CO_2^{\bullet-}$, see Section 3.2.2 of the main text). The strongest involvement of d_{z2} states into the chemical bonding is explained by their spatial compatibility with the lobes of the $6a_1$ and $4b_2$ molecular orbitals of $CO_2^{\bullet-}$.

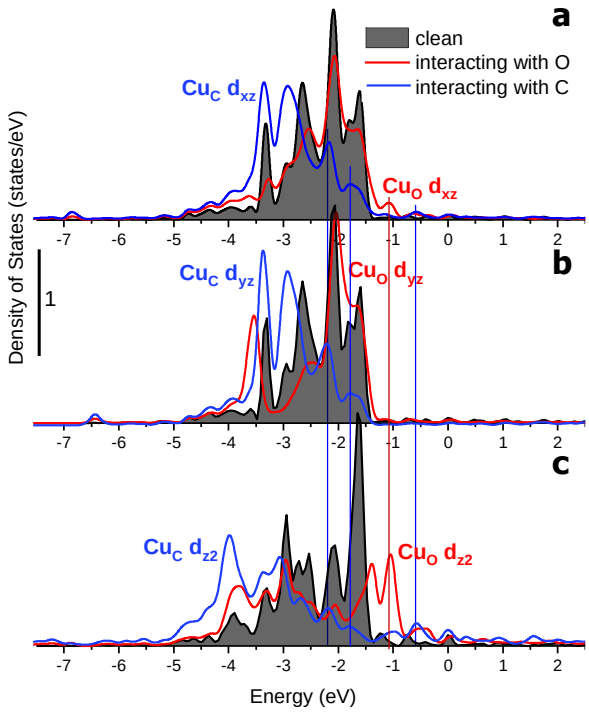

Figure S6. (**a,b**) d_π and (**c**) d_{z2} pDOS of the Cu atoms coordinating (blue line) C and (red line) O atoms of $*CO_2^-$ in (CO_2-$Na_{on\ top}$)/Cu(111). Grey filled areas mark the d states of these Cu atoms on clean Cu(111). Vertical lines show common d_π and d_{z2} states for of the Cu atom coordinating (blue) the C atom and (red) O atom of $*CO_2^-$.

The perturbation of the d_{yz} states of the O-coordinating Cu atom is explained by its hybridization with the perpendicular ($1a_2$) O lone pair of $CO_2^{\bullet-}$. In addition, the d_π electrons are rehybridized with the d_{z2} states. In fact, the d_{z2} and d_{xz} states of the O-coordinating Cu atom have a common resonance at −1.1 eV (red line in **Figure S6**). The d_{z2} and d_π states of the C-coordinating Cu atom have common resonances at −2.2, −1.8, and −0.6 eV (marked by blue lines in **Figure S6**). This effect has earlier been proposed to explain the bidirectional

redistribution of d electron density on the Pt atom participating in a dative bond with the O lone pair of adsorbed water molecule or hydroxyl.[8-9] It depopulates the d states overlapped with the close-shell orbitals into the available empty states to mitigate the strong Pauli repulsion from the O lone pair of H_2O, as a complementary mechanism to the "push-back" polarization of metal free electrons. This rehybridization can also alleviate the strong Pauli repulsion between the close-shell orbitals of $*CO_2^-$ and the surface, which may need further study.

Table S2. DFT-calculated vibrational frequencies of $*CO_2^-$ in the hydration-shared $*CO_2^-$ …Na^+ ion pair on Cu(111) simulated as (CO_2-$Na_{on\text{-}top}$+8H_2O) as compared with the corresponding experimental values from Ref.[10] (in brackets).

	Frequency, cm^{-1}
$\nu_{as}CO_2$	1460 (1515-1525)
$\nu_{s}CO_2$	1082 (1330)
δCO_2^-	750, 779 (703)
νCu-C	387 (345-350)

References

1. Ko, J.; Kim, B.-K.; Han, J. W., Density Functional Theory Study for Catalytic Activation and Dissociation of CO2 on Bimetallic Alloy Surfaces. *The Journal of Physical Chemistry C* **2016,** *120* (6), 3438-3447.
2. Cheng, T.; Xiao, H.; Goddard, W. A., Reaction Mechanisms for the Electrochemical Reduction of CO2 to CO and Formate on the Cu(100) Surface at 298 K from Quantum Mechanics Free Energy Calculations with Explicit Water. *Journal of the American Chemical Society* **2016,** *138* (42), 13802-13805.
3. Aresta, M.; Angelini, A., The Carbon Dioxide Molecule and the Effects of Its Interaction with Electrophiles and Nucleophiles. In *Carbon Dioxide and Organometallics*, Lu, X. B., Ed. 2016; Vol. 53, pp 1-38.
4. Janik, I.; Tripathi, G. N. R., The nature of the CO2- radical anion in water. *Journal of Chemical Physics* **2016,** *144* (15), 154307.

5. Aresta, M.; Dibenedetto, A.; Quaranta, E., State of the art and perspectives in catalytic processes for CO2 conversion into chemicals and fuels: The distinctive contribution of chemical catalysis and biotechnology. *Journal of Catalysis* **2016,** *343* (Supplement C), 2-45.
6. Aresta, M.; Dibenedetto, A.; Quaranta, E., Electronic Properties of CO_2. In *Reaction Mechanisms in Carbon Dioxide Conversion*, Springer: Heidelberg 2016; pp 2-7.
7. Gibson, D. H., Carbon dioxide coordination chemistry: metal complexes and surface-bound species. What relationships? *Coordination Chemistry Reviews* **1999,** *185-6*, 335-355.
8. Schiros, T.; Andersson, K. J.; Pettersson, L. G. M.; Nilsson, A.; Ogasawara, H., Chemical bonding of water to metal surfaces studied with core-level spectroscopies. *Journal of Electron Spectroscopy and Related Phenomena* **2010,** *177* (2-3), 85-98.
9. Schiros, T.; Takahashi, O.; Andersson, K. J.; Ostrom, H.; Pettersson, L. G. M.; Nilsson, A.; Ogasawara, H., The role of substrate electrons in the wetting of a metal surface. *Journal of Chemical Physics* **2010,** *132* (9).
10. Chernyshova, I. V.; Somasundaran, P.; Ponnurangam, S., On the origin of the elusive first intermediate of CO_2 electroreduction. *Proceedings of the National Academy of Sciences* **2018,** *115* (40), E9261-E9270.